

## Optical Absorption and Magnetic Circular Dichroism Studies of Hydrogen, Copper(II), Zinc(II), Nickel(II), and Cobalt(II) Crown Ether-substituted Monomeric and Dimeric Phthalocyanines†

Zbigniew Gasyna, Nagao Kobayashi, and Martin J. Stillman\*

Department of Chemistry, The University of Western Ontario, London, Ontario N5A 5B7, Canada

Monomeric and dimeric species of phthalocyanines with four, 15-crown-5-ether (1,4,7,10,13-pentaoxacyclopentadecane) voids at the 2,3 positions (ML) (where M = H<sub>2</sub>, Cu, Zn, Ni, or Co), have been studied using optical absorption and magnetic circular dichroism (m.c.d.) spectroscopies. The ready solubility of these crown ether-substituted complexes in chloroform allows the measurement of spectral data over a wide wavelength range. In particular, absorption and m.c.d. data are reported for H<sub>2</sub>L between 250 and 750 nm. The contribution by individual bands to the absorption and m.c.d. spectral envelopes measured for the monomeric and dimeric species of H<sub>2</sub>L and NiL, has been determined using deconvolution calculations carried out on pairs of related absorption and m.c.d. spectra. M.c.d. *A* terms have been used to identify the *Q*, *B*<sub>1</sub>, *B*<sub>2</sub>, and *N*  $\pi \rightarrow \pi^*$  degenerate transitions in the spectra of the monomer of NiL, at 14 946 cm<sup>-1</sup> (669 nm) in the visible region, and at 24 398 (410), 31 414 (318), and 36 286 cm<sup>-1</sup> (276 nm) in the u.v. region. The deconvolution calculations were also used to find the pairs of bands that arise from the exciton splittings in the *Q* and *B* bands of the cofacial dimers. In the spectra of the dimer of NiL, two degenerate bands are required to fit the observed envelope in the *Q*-band region [at 14 887 (672) and 15 832 cm<sup>-1</sup> (632 nm)], which indicates that the splitting is *ca.* 950 cm<sup>-1</sup>, while the pair of *B* bands are separated by *ca.* 2 180 cm<sup>-1</sup>. The deconvolution of the spectra of the H<sub>2</sub>L complex gives a value of 1 925 cm<sup>-1</sup> for the separation of the two components in the *B* band region.

Dimers of phthalocyanine molecules have been studied extensively over many years in both solution- and solid-state phases. In the solid state three polymorphic phases, the  $\alpha$ ,  $\beta$ , and  $\gamma$  forms, have been characterized by their unique X-ray powder pattern,<sup>1,2</sup> and have been studied by i.r.,<sup>1</sup> optical absorption,<sup>3</sup> and magnetic circular dichroism (m.c.d.)<sup>4</sup> spectroscopies. Reports of one-dimensional conductivity properties of Si-pc (pc = phthalocyaninate) aggregates<sup>5</sup> has led to increased interest in the aggregation and polymerization properties of the phthalocyanines.

The preparation of phthalocyanines with four 15-crown-5-ether (1,4,7,10,13-pentaoxacyclopentadecane) voids at the 2,3 positions, ML, provides an opportunity to study the dimerization phenomena of phthalocyanine complexes in solution.<sup>6,7</sup> The existence of well defined, rigidly cofacial dimeric species of these phthalocyanines<sup>6,7</sup> enables us to carry out spectroscopic studies, in some detail, of the interaction between the two large  $\pi$  systems.

The assignment of the absorption spectrum of the phthalocyanines is, in general, rather difficult because, with the exception of the lowest energy *Q* band near 660 nm, all the other bands, which are observed in the u.v. region, overlap significantly. Recently, we have identified five degenerate transitions between 750 and 240 nm (13 000–42 000 cm<sup>-1</sup>) in the spectra of Zn(pc) and Mg(pc) in methylene chloride solutions, by using band deconvolution calculations to estimate the actual number of bands that lie under the absorption and m.c.d. spectral envelopes.<sup>8,9</sup> By fitting both the absorption and the m.c.d. spectra with the same number of bands, and similar band centres and band widths, we reduce the ambiguity inherent in this technique.<sup>10</sup> These results can be compared with deconvolution calculations carried out on the dimeric,  $\alpha$ -phase phthalocyanine species formed as thin films on quartz disks following sublimation.<sup>4</sup> Spectroscopic studies of the crown-

substituted phthalocyanines offer a link between the solution phase monomeric species, like Zn(pc) and Mg(pc),<sup>8,9</sup> the solution phase binuclear phthalocyanines which exhibit dimer-like spectra,<sup>11,12</sup> and species prepared as thin films<sup>4</sup> which have the closely coupled geometry of the  $\alpha$ - and  $\beta$ -phase phthalocyanines. The effects of band doubling, and a general blue shift of the band maximum on passing from the monomeric to dimeric (and even polymeric) species in both the phthalocyanines and porphyrins in solution, as well as for the polymorphic and closely aggregated forms in the solid state, have been explained in terms of the exciton coupling of the  $\pi$  systems.<sup>4,11–13</sup>

In this paper, optical absorption and m.c.d. spectra are used in combination to characterize a number of crown phthalocyanine complexes. We report here deconvolution calculations for H<sub>2</sub>L and NiL, and the associated cofacial dimeric species formed in the presence of high concentrations of salt. We use the method of moments to compute the value of the magnetic moment for the *Q* band of both the monomeric and dimeric species.

### Experimental

**Materials and Methods.**—Chloroform (BDH) and methanol (Fisher) were Spectrograde. The crown phthalocyanines, ML, were prepared as described previously.<sup>6,7</sup> The phthalocyanines were dissolved in chloroform and the concentrations in solution were determined spectrophotometrically using the following

† Supplementary data available (No. SUP 56761, 4 pp.): calculated absorption and m.c.d. band positions. See Instructions for Authors, *J. Chem. Soc., Dalton Trans.*, 1989, Issue 1, pp. xvii–xx.

*Non-S.I. units employed:* B.M.  $\approx 9.274 02 \times 10^{-24}$  J T<sup>-1</sup>; D  $\approx 3.335 64 \times 10^{-30}$  C m.

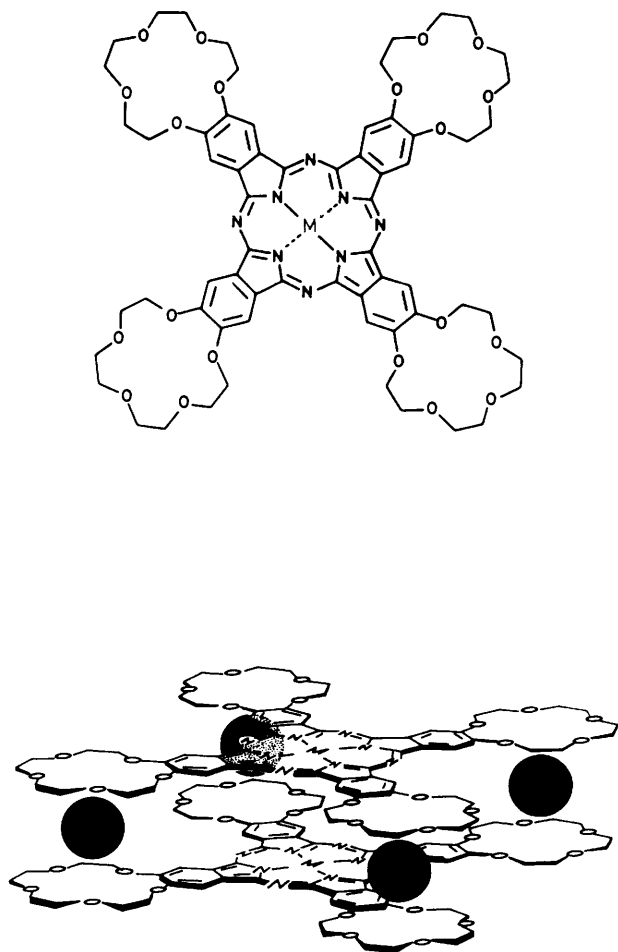


**Figure 1.** Structure of the crown phthalocyanine monomer and its cation-induced dimer (black circles indicate the position of the cations)

absorption coefficients:  $H_2L$ ,  $\epsilon = 33\,400\text{ dm}^3\text{ mol}^{-1}\text{ cm}^{-1}$  at 700 nm,  $ZnL$ ,  $96\,700\text{ dm}^3\text{ mol}^{-1}\text{ cm}^{-1}$  at 677 nm,  $CuL$ ,  $129\,400\text{ dm}^3\text{ mol}^{-1}\text{ cm}^{-1}$  at 676 nm,  $NiL$ ,  $70\,000\text{ dm}^3\text{ mol}^{-1}\text{ cm}^{-1}$  at 667 nm, and  $CoL$ ,  $59\,400\text{ dm}^3\text{ mol}^{-1}\text{ cm}^{-1}$  at 668 nm.<sup>7</sup> Dimerization was achieved following complexation with an excess of  $K^+$ . Typically,  $6 \times 10^{-5}\text{ dm}^3$  of a solution of  $CH_3CO_2K$  in chloroform, containing 10% (v/v) of methanol, was added to solutions of either  $H_2L$  or  $ML$  in chloroform ( $ML$  concentration about  $1 \times 10^{-5}\text{ mol dm}^{-3}$ ) to give a final  $[K^+]/[ML]$  ratio in the range 3–20:1. There was little additional effect on either the absorption or m.c.d. spectrum once the ratio exceeded 2:1 in accordance with previous reports.<sup>7</sup>

Absorption spectra were obtained with a CARY model 219 spectrophotometer. M.c.d. spectra were obtained with a JASCO J-500C spectropolarimeter controlled by an IBM Instruments S9001 computer using the computer program CDSCANS.<sup>14</sup> The magnetic field of 5.5 T was provided by an Oxford Instruments SM2 superconducting magnet operating at room temperature. The magnetic field strength and sign were calibrated using the visible-region band of aqueous  $CoSO_4$ , for which a value of  $\Delta\epsilon_M = -1.897 \times 10^{-2}\text{ dm}^3\text{ mol}^{-1}\text{ cm}^{-1}\text{ T}^{-1}$  at 510 nm was calculated.

*Spectral Analysis of the Absorption and M.C.D. Data.*—All experimental spectra shown in this paper were automatically digitized as they were recorded. Each spectrum has had the appropriate baselines subtracted. Absorption spectra have been

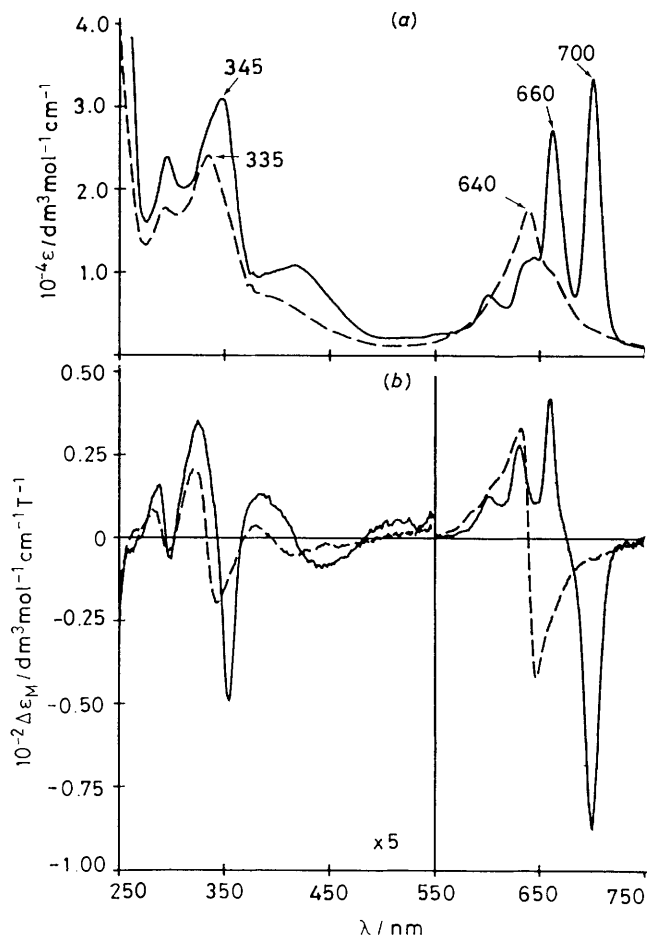


**Figure 2.** Optical absorption (a) and m.c.d. (b) spectra of  $H_2L$  (solid line) and its dimeric species (broken line) formed in  $CHCl_3$  by the addition of  $CH_3CO_2K$  in  $CHCl_3$  containing 0.1% (v/v) of methanol.  $[CH_3CO_2K]/[H_2L] = 3.0$

recalculated in units of  $\epsilon$  ( $\text{dm}^3\text{ mol}^{-1}\text{ cm}^{-1}$ ) and the m.c.d. spectra are presented as  $\Delta\epsilon_M$  ( $\text{dm}^3\text{ mol}^{-1}\text{ cm}^{-1}\text{ T}^{-1}$ ). Computer programs developed for use with the IBM S9001 laboratory microcomputer were applied for the analysis of the optical absorption and m.c.d. spectra envelopes, and also for subsequent plotting. The absorption and m.c.d. spectra were fitted with Gaussian bands using the program SIMPFIT.<sup>10</sup> The moments analysis was carried out by direct integration of the digitized absorption and m.c.d. spectra. The theoretical m.c.d. expressions for allowed electronic transitions were taken from Schatz and co-workers.<sup>15,16</sup> The spectral data were manipulated and plotted on an HP 7550A plotter using the data base management program Spectra Manager.<sup>17</sup>

## Results and Discussion

*(1) Absorption and M.C.D. Spectra of the Monomeric and Dimeric ML Complexes.*—Figure 1 shows the structure of the crown phthalocyanine monomer and its cation-induced dimer (black circles indicate the position of the added cations). Because of the structural constraints, the dimer is assumed to be in a completely eclipsed, cofacial conformation.<sup>6,7</sup>

Figures 2–6 show optical absorption and m.c.d. spectra of the crown ether-substituted phthalocyanines:  $H_2L$ ,  $CuL$ ,  $ZnL$ ,  $NiL$ , and  $CoL$  (depicted as solid lines), and their dimeric derivatives (marked as broken lines) formed in  $CHCl_3$  upon addition of an excess of  $K^+$ ,<sup>6,7</sup> respectively. The excellent u.v.-

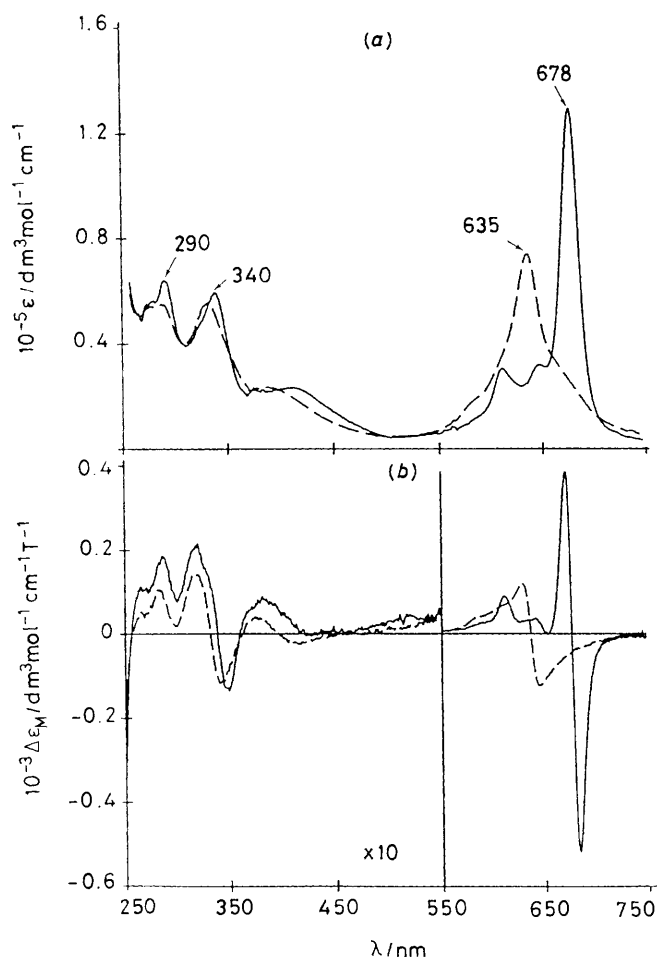


**Figure 3.** Optical absorption (a) and m.c.d. (b) spectra of CuL (solid line) and its dimeric species (broken line) formed in  $\text{CHCl}_3$ . Details as in Figure 2, with  $[\text{CH}_3\text{CO}_2\text{K}]/[\text{CuL}] = 12.0$

transmitting properties of the chloroform solvent allow us to report spectral data that were previously unavailable for  $\text{H}_2\text{pc}$ ,  $\text{Cu}(\text{pc})$ , and  $\text{Ni}(\text{pc})$  because these phthalocyanine species are so insoluble in u.v.-transmitting solvents.

Of the five complexes studied in this work, the absorption and m.c.d. spectra of  $\text{H}_2\text{L}$  are the most different because of the effects of the  $D_{2h}$  symmetry imposed on the  $\pi$  system by the two hydrogens.<sup>18,19</sup> The m.c.d. spectrum of  $\text{H}_2\text{L}$  [solid line in Figure 2(b)] shows, in the  $Q$ -band region (700 nm), a set of bands that are characteristic of a  $D_{2h}$  phthalocyanine complex.<sup>20-22</sup> The m.c.d.  $B$  terms<sup>15,16,23,24</sup> at 701 (14 270) and 661 nm (15 120  $\text{cm}^{-1}$ ) identify non-degenerate transitions to the split  $e_g \pi^*$  lowest unoccupied molecular orbital (l.u.m.o.) which has split at the lower symmetry of the  $D_{2h}$   $\text{H}_2\text{L}$  species, to give two bands labelled  $Q_x$  and  $Q_y$ , respectively.<sup>18,21</sup> While the band centres and widths of the  $Q_x$  and  $Q_y$  components for  $\text{H}_2\text{L}$  are quite similar to those for  $\text{H}_2\text{pc}$  in dimethylacetamide (dma)<sup>20</sup> and 1-chloronaphthalene,<sup>21</sup> the Soret region bands are unlike those measured for  $\text{H}_2\text{pc}$ <sup>20</sup> in dma. The prominent band at about 410 nm (24 400  $\text{cm}^{-1}$ ), associated with a broad, derivative feature in the m.c.d. spectrum [Figure 2(b)], is seen for all the ML species to different extents. The spectral features for the  $\text{H}_2\text{L}$  in this region indicate that the derivative-shaped band is made up from the overlap of oppositely signed  $B$  terms.

In studies on  $\text{Zn}(\text{pc})$ ,<sup>8</sup>  $\text{H}_2(\text{pc})$ ,<sup>20</sup> and  $\text{Li}_2(\text{pc})$ ,<sup>21</sup> we have noted that there are bands (characterized by  $A$  terms in the m.c.d. spectrum) that can red-shift out of the main Soret band envelope which is centred on 330 nm. In our previous studies we have

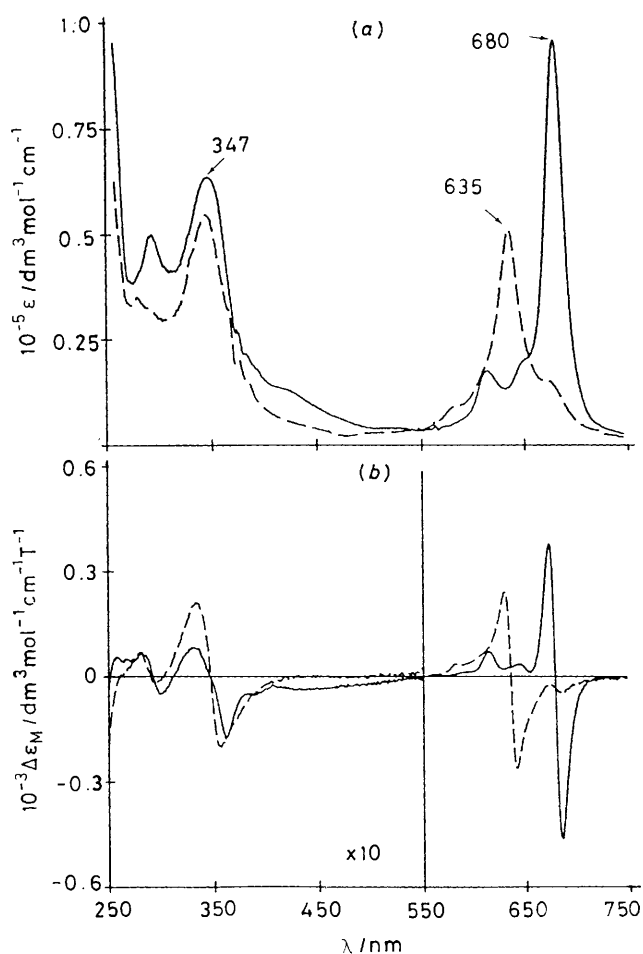


**Figure 4.** Optical absorption (a) and m.c.d. (b) spectra of ZnL (solid line) and its dimeric species (broken line). Details as in Figure 2, with  $[\text{CH}_3\text{CO}_2\text{K}]/[\text{ZnL}] = 10.5$

associated this spectral effect with changes in the axial ligation of the central metal. In the case of phthalocyanines with crown ether substituents, it is possible that perturbations to the phthalocyanine  $\pi$  ring result in the same effect. The m.c.d. spectrum for  $\text{NiL}$  indicates that the transition responsible for the band at 410 nm (24 400  $\text{cm}^{-1}$ ) is degenerate in nature.

Addition of two or more mole equivalents of  $\text{K}^+$  to monomeric  $\text{H}_2\text{L}$  results in formation of the dimer.<sup>7</sup> Clearly, the whole spectrum blue-shifts (Figure 2), with the main  $Q$  band now centred at 640 nm. Like the spectrum of the weakly coupled  $\alpha\text{-H}_2\text{pc}$ ,<sup>25</sup> the effect of dimerization is to increase the symmetry for the group orbitals that span the whole dimer from the  $D_{2h}$  of the  $\text{H}_2\text{L}$  monomer. Thus a derivative feature is now observed. In view of the similarity between the m.c.d. spectra of dimeric  $\text{H}_2\text{L}$  and the metallated complexes in the  $Q$ -band region, we assign this band for the dimeric  $\text{H}_2\text{L}$  as an  $A$  term, in accordance with the assignment made for the  $\alpha\text{-H}_2\text{pc}$  thin film.<sup>25</sup> The deconvolution calculations, see below, support this assignment. A mechanism to account for this effect is suggested from work by Lever and co-workers<sup>12</sup> in which deprotonation of a dimeric metal free pc species in solution resulted in the loss of the normal  $D_{2h}$  spectrum, a single  $D_{4h}$ -like  $Q$  band was then observed. The data for the dimeric  $\text{H}_2\text{L}$  might arise if the two protons move from the off-axis positions of the monomer. We should note that the m.c.d. spectra of  $\text{Li}_2(\text{pc})$  are typical of an  $\text{M}(\text{pc})$  species, the symmetry is clearly  $D_{4h}$  not  $D_{2h}$ ,<sup>21</sup> as it might be suggested by the presence of two Li atoms.

The absorption and m.c.d. spectra of the metal-substituted

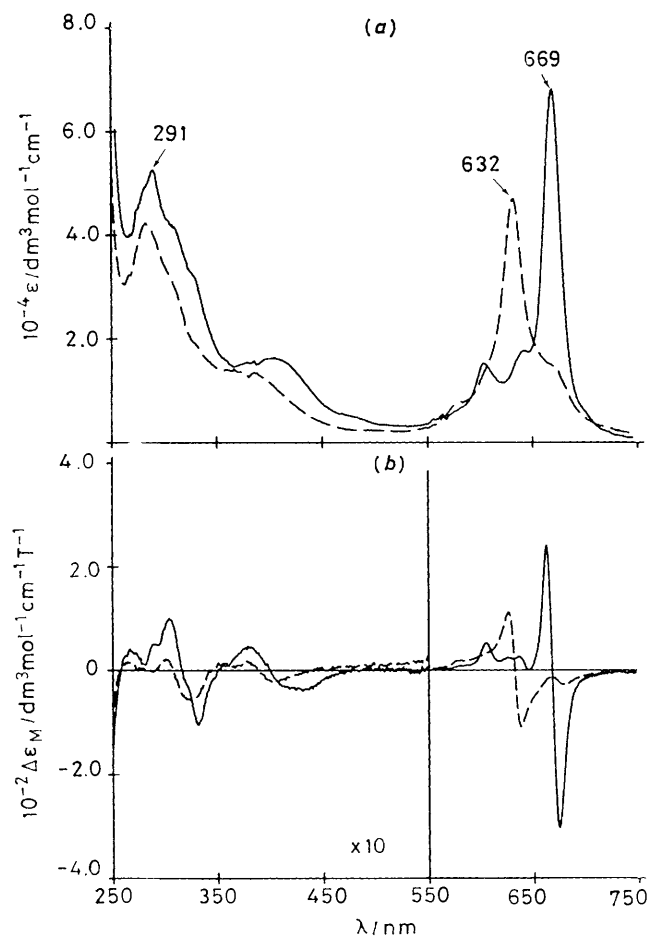


**Figure 5.** Optical absorption (a) and m.c.d. (b) spectra of NiL (solid line) and its dimeric species (broken line). Details as in Figure 2, with  $[\text{CH}_3\text{CO}_2\text{K}]/[\text{NiL}] = 5.1$

crown phthalocyanines, CuL, ZnL, NiL, and CoL (solid lines in Figures 3, 4, 5, and 6, respectively), show spectral envelopes characteristic of monomeric,  $D_{4h}$  phthalocyanine complexes.<sup>8,21,22</sup> The m.c.d. spectra of these complexes show the presence of a distinctive m.c.d. *A* term in the *Q*-band region located near 670 nm in each case. This indicates that the *Q* band results from a degenerate transition as expected.<sup>18,19</sup> The vibrational overtone bands at shorter wavelengths are a typical feature of the M(pc) complexes. Deconvolution always indicates a series of weak, positive m.c.d. *B* terms in this region<sup>8</sup> (cf. Figure 9).

The spectral region between 500 and 250 nm is much more complicated than the visible region, even for the ZnL complex, in which no charge transfer is to be expected between the metal and the  $\pi$  ring. Although the m.c.d. spectra reveal more detail than the absorption spectra for each complex, determination of the individual band centres requires full spectral envelope deconvolution (cf. Figure 9 for NiL). We will return to a discussion of the assignment of the observed bands in the Soret region below.

The absorption and m.c.d. spectra of the dimeric ML complexes formed in the presence of an excess of  $\text{K}^+$  ions are shown as broken lines in Figures 3, 4, 5, and 6 for CuL, ZnL, NiL, and CoL, respectively. Both the optical absorption and these m.c.d. spectra of the dimeric species share a number of common features. The most important are: (i) the *Q* band lies at higher energy with decreased intensity and retains the character of a degenerate transition, (ii) the changes in the u.v. region are less distinctive, with the blue shift significantly less pronounced, (iii) the spectra of dimeric species formed from either a metal-

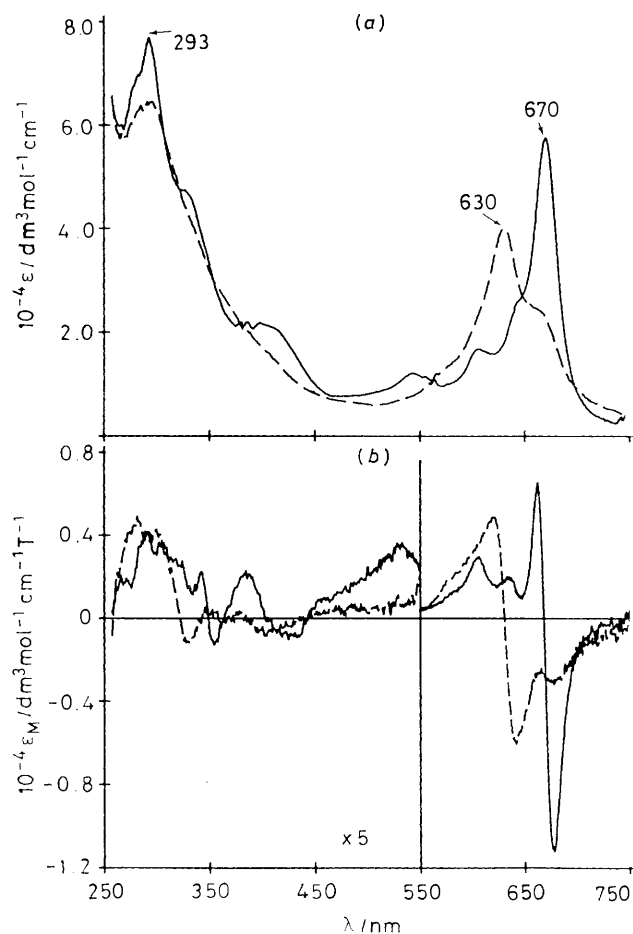


**Figure 6.** Optical absorption (a) and m.c.d. (b) spectra of CoL (solid line) and its dimeric species (broken line). Details as in Figure 2, with  $[\text{CH}_3\text{CO}_2\text{K}]/[\text{CoL}] = 13.0$

substituted phthalocyanine with  $D_{4h}$  symmetry, or from the metal-free phthalocyanine with  $D_{2h}$  symmetry, reflect a similar, apparently  $D_{4h}$  symmetry, and (iv) the absorption and m.c.d. spectra in the visible region show distinct spectral features at lower energy than the main transition. The assumption is made here that these spectral features arise from forbidden transitions<sup>11,13</sup> of the exciton split pair of *Q* bands, where transitions to  $Q^+$  are allowed but to  $Q^-$  are forbidden.

(2) *Deconvolution of the Absorption and M.C.D. Spectra of the Monomeric and Dimeric  $\text{H}_2\text{L}$  Complexes.*—A detailed spectral deconvolution analysis of the absorption and m.c.d. spectra was carried out for  $\text{H}_2\text{L}$ , its cofacial dimer species,  $(\text{H}_2\text{L})_2$ , NiL and its cofacial dimer species,  $(\text{NiL})_2$ , using the techniques described previously for Zn(pc)<sup>8</sup> and Mg(pc).<sup>9</sup> Figure 7 shows the results of the deconvolution of the monomeric  $\text{H}_2\text{L}$  spectra in the visible and u.v. regions. The parameters that describe the bands calculated in these regions are presented in SUP 56761.

Figure 8 shows the results of the deconvolution of the  $(\text{H}_2\text{L})_2$  spectra in the visible and u.v. regions. The m.c.d. spectrum shows that there is significant overlap of a negative *B* term (a vibronic component of the  $Q_x$ ) in the region of  $Q_y$  (o-o). As a result the intensity of the *B* term corresponding to  $Q_y$  (o-o) is greatly diminished. The fitting program cannot reproduce this effect. The parameters that describe the bands calculated in these regions are presented in SUP 56761. The splitting of both the *Q* and *B* bands is due to the exciton coupling phenomenon.<sup>4,6,7,11,12</sup> Such splittings can be calculated from the analysis of the m.c.d. spectral envelope by locating the pairs of *A*

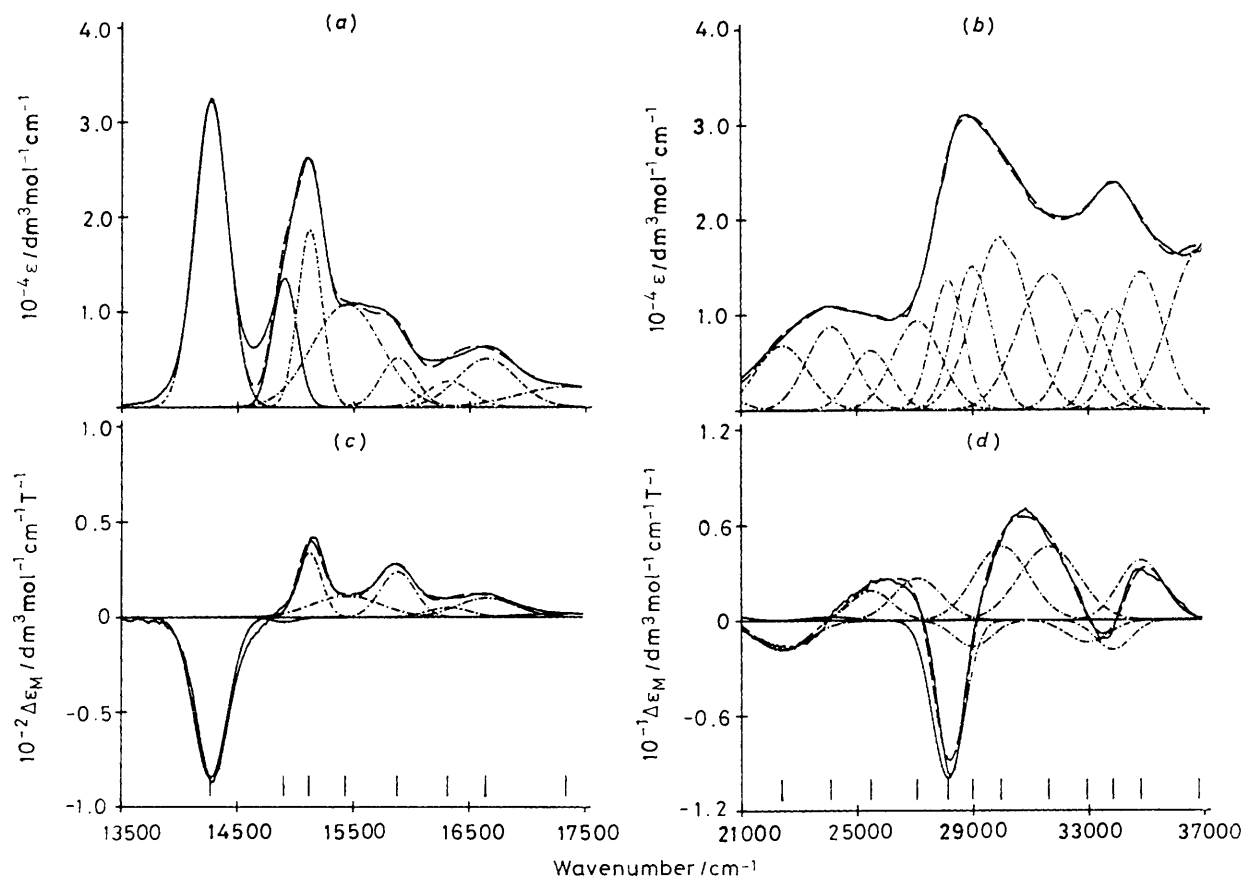


**Figure 7.** Band analysis for  $H_2L$  in  $CHCl_3$ : optical absorption (*a,b*); (—) experimental data, (---) fitted data, (-·-·-) individual bands; m.c.d. (*c,d*); (—) experimental data, (---) fitted data, (-·-·-) bands. The vertical lines show the band centre positions

terms. For the  $(H_2L)_2$  species there is only one distinct  $A$  term in the  $Q$ -band region. The fit in the  $Q$ -band region was difficult to accomplish. With the restriction imposed by the absorption and m.c.d. components, only an  $A$  term could be used at  $15\,596\text{ cm}^{-1}$ . So little m.c.d. intensity was observed at  $14\,000\text{ cm}^{-1}$  that the bands used in the fit had no significance. However, the  $B$  transition exhibits noticeable splitting of  $1\,925\text{ cm}^{-1}$ .

(3) *Deconvolution of the Absorption and M.C.D. Spectra of the Monomeric and Dimeric NiL Complexes.*—Figure 9 shows the results of the deconvolution of the NiL spectra in the visible and u.v. regions. The fitting parameters used that describe the transitions calculated in these regions are presented in SUP 56761. Figure 10 shows the results of the deconvolution of the  $(NiL)_2$  spectra in the visible and u.v. regions. The parameters that describe the bands calculated in these regions are presented in SUP 56761. The effect on the m.c.d. spectra of dimerization is to double up the number of transitions, as the exciton coupling results in a pair of transitions, one forbidden, the other allowed.<sup>4,11,13</sup> Both of these transitions are expected to be degenerate.<sup>4</sup> Thus, in the visible region of the m.c.d. spectrum of dimeric NiL, we observe a weak band at  $14\,887\text{ cm}^{-1}$  and a stronger allowed transition to higher energy at  $15\,832\text{ cm}^{-1}$ . Identification of this pair of transitions yields a splitting of about  $950\text{ cm}^{-1}$ . Although this assignment is based on observing a 'forbidden' transition, the lack of intensity in the low energy component is in accord with a forbidden band that gains intensity from the strong vibronic coupling present already in the  $Q$  band of phthalocyanine.

We have considered carefully whether the band at  $14\,887\text{ cm}^{-1}$  is a contribution from unreacted, residual monomer

species. Attempts to subtract a contribution of the monomer spectrum from the dimer spectrum however do not eliminate this particular band. Indeed new and quite different features are introduced into the spectrum. A similar result is obtained when comparing the spectra of  $H_2L$  and its dimeric species. We conclude that the bands on the red side of the main  $Q$  band (dimer) are entirely related to the dimer and have an origin in transitions to the 'forbidden' exciton component.

Analysis of the  $B$  region requires two  $A$  terms between  $25\,000$  and  $28\,000\text{ cm}^{-1}$ , which we characterize as the pair of bands arising from the split  $B$  band. While the  $B$  band of the monomer is exceptionally low in energy (at  $24\,398\text{ cm}^{-1}$ ), the split  $B$  band for the NiL dimer is found in the more usual position, at  $25\,372$  and  $27\,550\text{ cm}^{-1}$ . However, a low energy for the  $B$  band is found for the dimer of the metal-free species,  $H_2L$ . As for the  $D_{4h}pc^{2-}$  species,<sup>20</sup> we observe the pair of split  $B$  bands at an unusually low energy (at  $23\,384$  and  $25\,309\text{ cm}^{-1}$ ). These findings suggest that there is a strong effect on the  $\pi$  ring excited states when there are external substituents such as crown ethers attached to the periphery of the phthalocyanine ring. These values, and the values obtained for  $(H_2L)_2$ , can be compared to values of  $2\,000$ – $3\,000\text{ cm}^{-1}$  calculated in both regions for the  $\alpha$ -polymorphic form of phthalocyanines<sup>4</sup> and to values of  $770$ – $1\,600\text{ cm}^{-1}$  calculated on the basis of e.s.r. data for the crown phthalocyanines.<sup>7</sup>

The results of the deconvolution calculations of the absorption and m.c.d. spectra of the  $H_2L$  and NiL species are summarized in Table 1, and in SUP 56761.

The results of the moment analysis of the m.c.d. and absorption spectra of the  $Q$  band of the  $H_2L$  and NiL species are shown in Table 2. It has been indicated<sup>8</sup> that the fitting procedure underestimates the absolute value of the magnetic

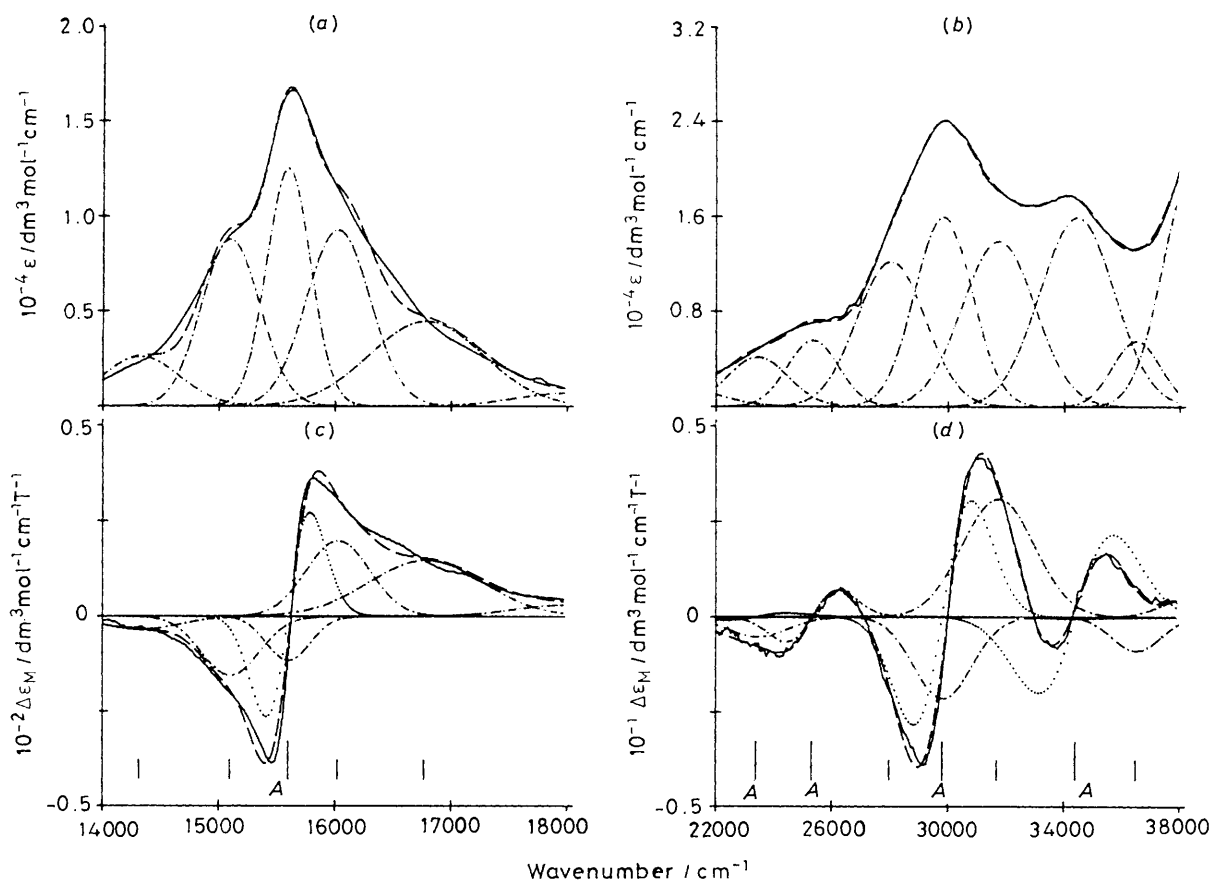


**Figure 8.** Band analysis for  $(\text{H}_2\text{L})_2$  in  $\text{CHCl}_3$ : optical absorption (*a,b*); (—) experimental data, (---) fitted data, (· · · · ·) individual bands; m.c.d. (*c,d*); (—) experimental data, (---) fitted data, (· · · · ·) *A* terms, (---) *B* terms. The vertical lines show the band centre positions; the line corresponding to the *A* term is labelled *A*

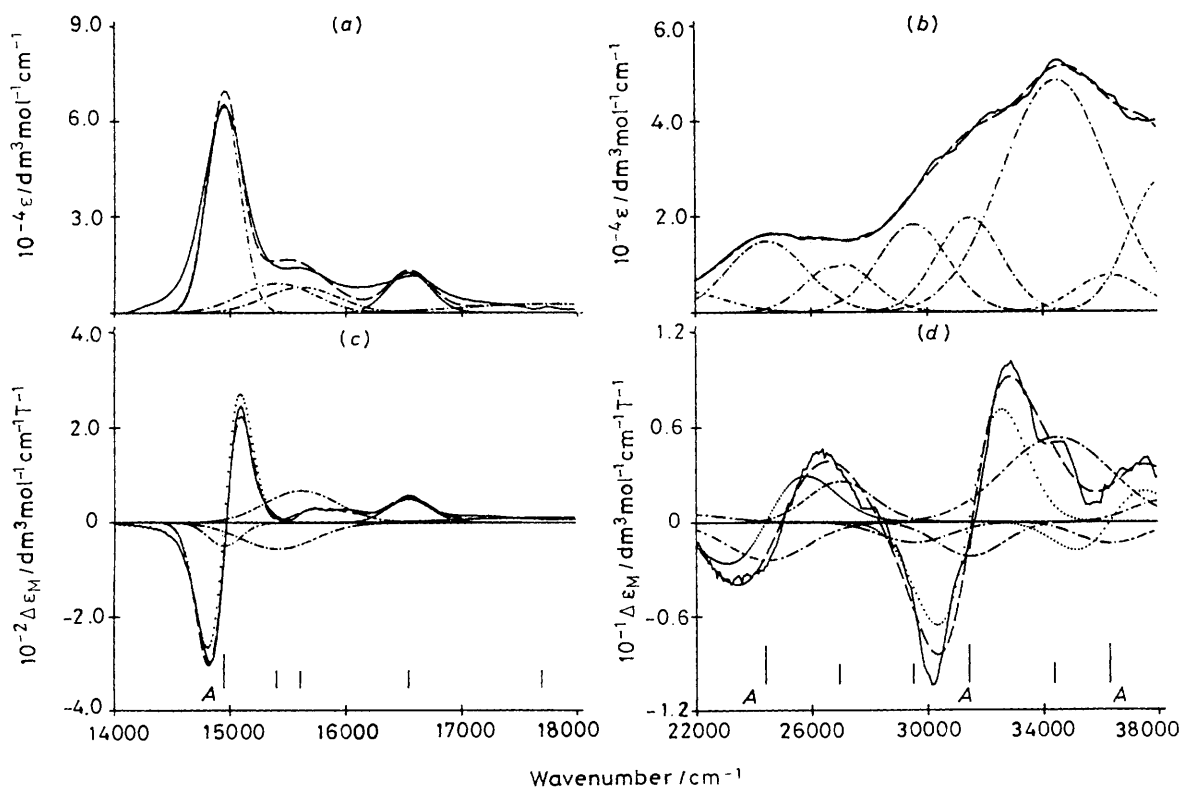


**Figure 9.** Band analysis for  $\text{NiL}$  in  $\text{CHCl}_3$ ; details as in Figure 8

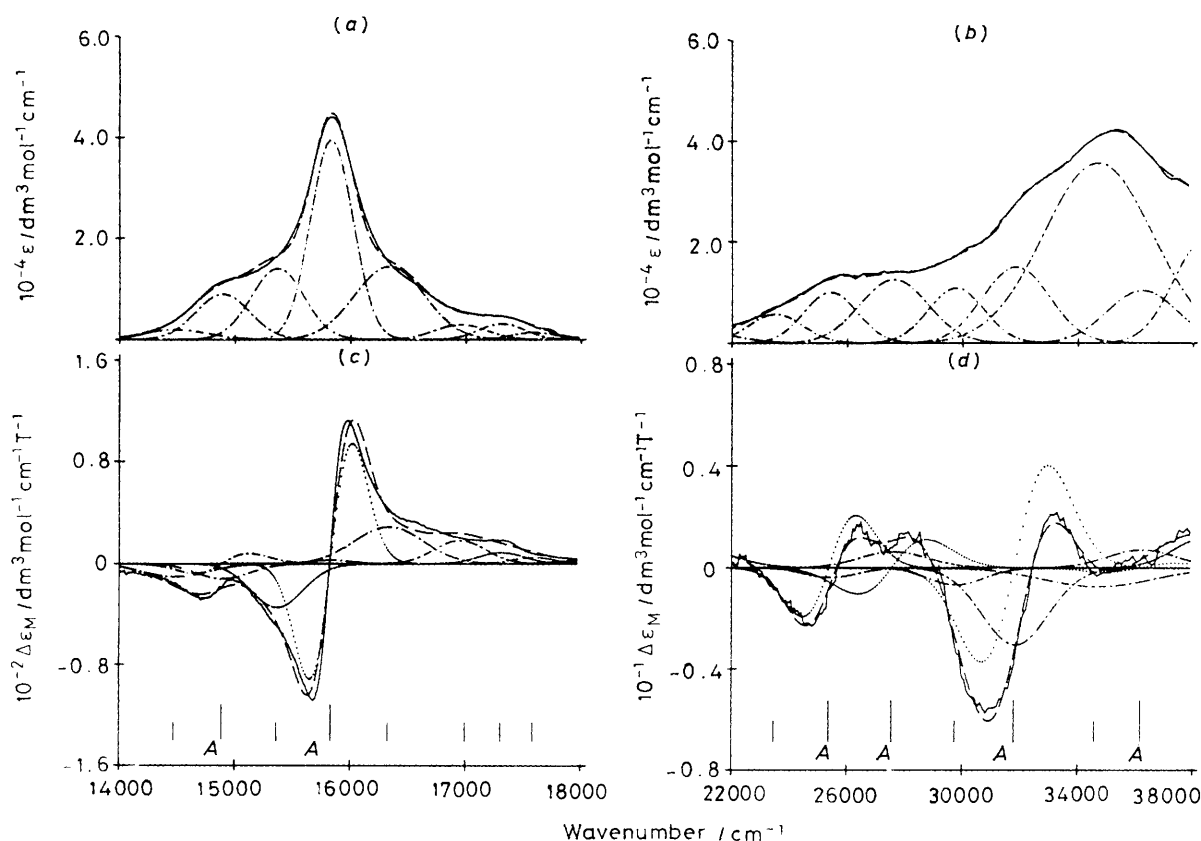


Figure 10. Band analysis for  $(\text{NiL})_2$  in  $\text{CHCl}_3$ ; details as in Figure 8

Table 1. Band energies obtained by fitting of the spectra of  $\text{H}_2\text{L}$ - and Ni-substituted crown ether phthalocyanines and their dimer species in chloroform solution. Bands exhibiting the m.c.d.  $A$  terms are indicated ( $A$ )

$\text{H}_2\text{L}$ $\nu/\text{cm}^{-1}$ ( $\lambda/\text{nm}$ )	$(\text{H}_2\text{L})_2$ $\nu/\text{cm}^{-1}$ ( $\lambda/\text{nm}$ )	$\text{NiL}$ $\nu/\text{cm}^{-1}$ ( $\lambda/\text{nm}$ )	$(\text{NiL})_2$ $\nu/\text{cm}^{-1}$ ( $\lambda/\text{nm}$ )
14 270 (701)	14 315 (699)	(A) 14 946 (669)	14 473 (691)
14 902 (671)	15 095 (662)	15 400 (649)	(A) 14 887 (672)
15 120 (661)	(A) 15 596 (641)	15 606 (641)	15 361 (651)
15 432 (648)	16 021 (624)	16 541 (605)	(A) 15 832 (632)
15 879 (630)	16 765 (596)	17 692 (565)	16 326 (613)
16 314 (612)	17 988 (556)		16 945 (590)
16 643 (601)			17 304 (578)
17 337 (577)			17 583 (569)
			17 993 (556)
19 781 (506)	20 668 (484)	21 256 (470)	20 507 (488)
22 390 (447)	(A) 23 384 (428)	(A) 24 398 (410)	23 462 (426)
24 079 (415)	(A) 25 309 (395)	26 944 (371)	(A) 25 372 (394)
25 466 (393)	27 981 (357)	29 482 (339)	(A) 27 550 (363)
27 058 (370)	(A) 29 799 (336)	(A) 31 414 (318)	29 736 (336)
28 128 (356)	31 678 (316)	34 355 (291)	(A) 31 798 (314)
28 974 (345)	(A) 34 388 (291)	(A) 36 286 (276)	34 576 (289)
29 957 (334)	36 481 (274)	38 086 (263)	(A) 36 173 (276)
31 596 (316)	38 442 (260)		38 332 (261)
32 928 (304)			
33 826 (296)			
34 785 (287)			
36 803 (272)			

moment for the  $Q$  band because the whole transition is not included. This effect has been also seen here by comparison of data in SUP 56761 (data obtained by fitting) and Table 2 (data obtained by numerical integration over the whole  $Q$ -band

region). The same integration program has been used to calculate angular momentum values for complexes of  $\text{Zn}(\text{pc})$ .<sup>8</sup> By expressing the magnetic moment in terms of the  $A_1/D_0$  values we can remove any effects of uncertainty in the estimation of the concentrations in a range of complexes. For the  $Q$  band, we find an  $A_1/D_0$  value for monomeric  $\text{NiL}$  of 3.5, for the dimer 3.3, and for  $(\text{H}_2\text{L})_2$  3.5. For  $\text{Zn}(\text{pc})$ , we found<sup>8</sup> a considerable ligand dependence, with a range from 1.5 (for the imidazole complex) to 3.5 (for the cyanide complex). This ligand dependence of the excited state magnetic moment has been discussed previously for a series of metallophthalocyanine complexes,<sup>21</sup> and has been associated with the extent of coupling between the ring  $\pi$  and metal orbitals. Larger magnetic moments are observed for axial ligands that have strong  $\pi$  acceptor properties, while lower values are observed with ligands with strong  $\sigma$  donor properties. In addition, both the shape of the m.c.d. band envelope, and the calculated angular momentum, are changed significantly when charge-transfer bands lie at this same energy. For  $\text{NiL}$ , we associate a value for  $A_1/D_0$  of 3.5 with a decoupled metal- $\pi$  ring system, a situation comparable with  $(\text{CN})\text{Zn}(\text{pc})$ .<sup>8</sup> Despite the broadening that accompanies dimerization in the  $Q$ -band region, integration over the whole band can overcome this problem and provide usable angular momentum data. As is shown in Table 2, the value of the  $Q$ -band angular momentum for the dimeric species does not diminish.

(4) Comparison between Band Energies Observed for  $\text{NiL}$ ,  $\text{Mg}(\text{pc})$  and  $\text{Zn}(\text{pc})$ .—The first five singlet excited states in phthalocyanine complexes have been described by Gouterman and co-workers<sup>18,19</sup> (with the more recent addition of the  $B_1$  and  $B_2$  subdivision)<sup>4,8,9</sup> as  $Q$ , ( $B_1$ ,  $B_2$ ),  $N$ ,  $L$ , and  $C$ , ranging in energy from 15 000 to about 50 000  $\text{cm}^{-1}$  (700–200 nm). As each of these states is degenerate in species that exhibit  $D_{4h}$

**Table 2.** Moments analysis of the *Q*-band absorption and m.c.d. spectra of the crown ether phthalocyanine complexes:  $H_2L$ ,  $(H_2L)_2$ ,  $(NiL)$ , and  $(NiL)_2$ 

Complex	$\nu/cm^{-1}$ ( $\lambda/nm$ )	$D_0^a$	$\langle\Delta\epsilon_M\rangle_1^b$	$A_1^c$	$A_1/D_0$	$\mu^d$	$\langle\Delta\epsilon_M\rangle_0^b$	$10^3 B_0^c$	$10^4 B_0/D_0$
$H_2L$	15 399 (649)	8.5					0.34	2.22	2.63
$(H_2L)_2$	15 798 (633)	5.5	2 930	19.2	3.48	3.25	0.43	2.85	5.16
$NiL$	15 561 (643)	12.6	6 680	43.8	3.48	3.25	1.01	6.60	5.24
$(NiL)_2$	15 786 (633)	10.9	5 420	35.6	3.26	3.04	-0.31	-2.02	-1.85

<sup>a</sup>  $D_0$  is the dipole strength in units of  $D^2$  ( $D$  = Debye units), see ref. 16, p. 537. <sup>b</sup>  $\langle\Delta\epsilon_M\rangle_1$  is the first moment and  $\langle\Delta\epsilon_M\rangle_0$  is the zeroth moment. <sup>c</sup> The units of  $A_1$  are  $D^2$ , the units of  $B_0$  are  $D^2$  cm; see ref. 16, p. 537. <sup>d</sup>  $\mu$  = magnetic moment in units of B.M.,  $\mu_B$ , calculated as  $2(A_1/D_0) \times 0.4669$ .

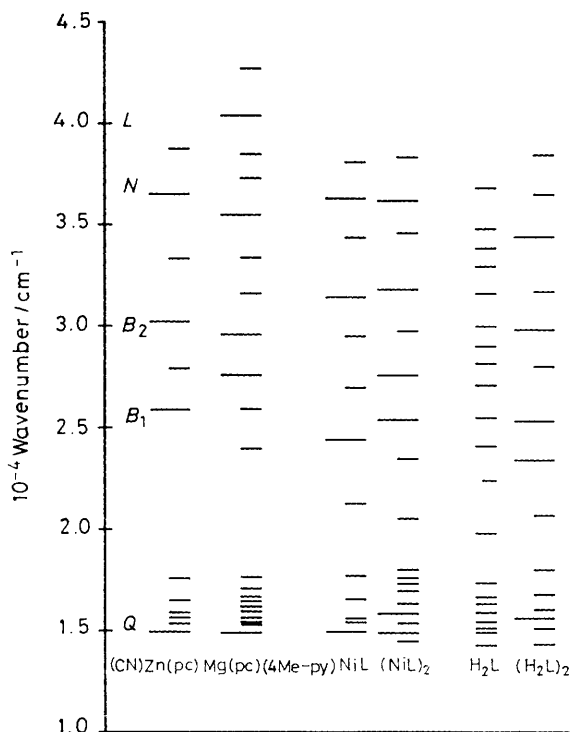


**Figure 11.** Comparison between energies of transitions calculated from the spectra of  $NiL$  to  $Zn(pc)$  and  $Mg(pc)$ . Longer lines denote degenerate transitions (m.c.d.  $A$  terms), letters indicate approximate positions of the theoretically calculated  $Q$ ,  $B_1$ ,  $B_2$ ,  $N$ , and  $L$  bands

symmetry, we should be able to identify the spectral bands that arise from transitions to these excited states in our spectra, because m.c.d.  $A$  terms are predicted to be observed. However, while  $A$  terms are clearly distinguishable under the  $Q$  band at 700 nm, it is much more difficult to sort out the origin of the bands in the u.v. region. Deconvolution calculations are the only way to find the number and location of the  $A$  terms that make up the spectral envelope in the 400–220 nm region. The conclusion that we reached when we compare the location of  $A$  terms in the m.c.d. spectrum with band maxima in the absorption spectrum is that the wavelength of the band maxima obtained directly from the absorption spectrum *does not* give the correct wavelengths for the degenerate transitions that are associated with the  $B_1$ ,  $B_2$ ,  $N$ , and  $L$  transitions. Unlike the rather simpler situation in porphyrin spectra, we cannot assign the  $B$  band in phthalocyanines to the absorption band with the greatest absorption near 350 nm.

Figure 11 compares the energies of the transitions calculated from the spectra of monomeric and dimeric  $NiL$  with transition energies calculated for  $Zn(pc)$ <sup>8</sup> and  $Mg(pc)$ .<sup>9</sup> The long lines in Figure 11 represent degenerate transitions which are identified by  $A$  terms used to fit the m.c.d. spectral envelopes. The shorter lines were fitted with  $B$  terms in the m.c.d. spectrum, and we

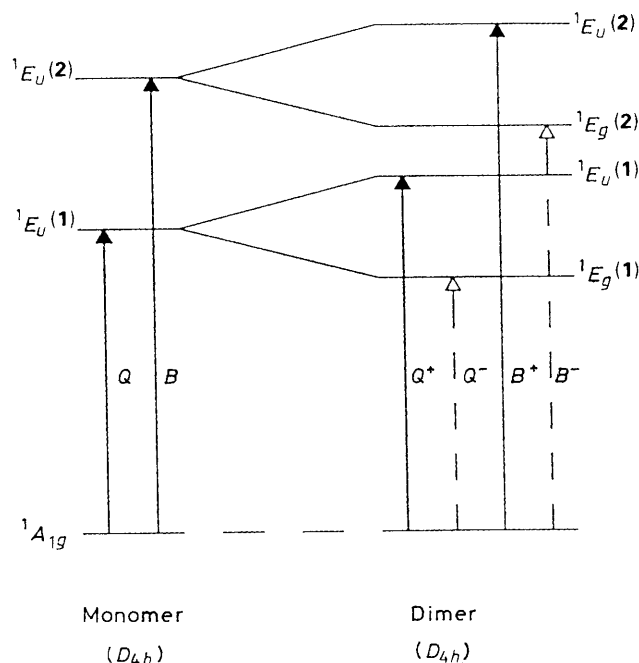


**Figure 12.** Orbital diagram for exciton coupling in a phthalocyanine dimer with  $D_{4h}$  geometry. The solid line and broken line arrows mark allowed and forbidden transitions, respectively (diagram taken from refs. 12 and 13)

characterize these transitions as being non-degenerate in nature. We find four degenerate bands, using the fitting techniques, in the spectra of monomeric  $NiL$ , at 14 946, 24 398, 31 414, and 36 286  $cm^{-1}$ . Data from deconvolution calculations carried out on the spectra of the  $\alpha$  polymorph of thin films of  $M(pc)$  species on quartz plates,<sup>4</sup> and of a range of ligated species in solution, including  $Li_2(pc)$ ,<sup>21</sup>  $Zn(pc)$ ,<sup>8,22</sup>  $Mg(pc)$ ,<sup>9</sup> and even the  $D_{4h} pc^{2-}$  species,<sup>20</sup> show that there can be considerable variation in the energy of the  $B$  band defined as the transition to the second degenerate state, nominally an orbital transition,<sup>18</sup>  $a_{2u} \rightarrow e_g$ . In all cases,<sup>8,9,22</sup> a degenerate transition is observed in the 24 000–28 000  $cm^{-1}$  region. For  $pc^{2-}$ ,  $(CN)_2Li_2(pc)$ , and  $(CN)Zn(pc)$  the  $B$  band is red-shifted to such an extent that it is clearly discernible on the side of the broader absorption to higher energy; the energy of the  $B$  band of the  $(CN)Zn(pc)$  species lies at a much lower energy (25 874  $cm^{-1}$ ) than the  $B$  bands of other  $Zn(pc)$  complexes.<sup>8</sup> Therefore, we are not surprised to find that for the  $NiL$  species, the  $B$  band is rather lower in energy, and therefore, more prominent, than is normally observed for  $M(pc)$  complexes in general. Similarly, while the  $N$  and  $L$  bands are quite clearly identifiable in the spectra of both  $Zn(pc)$ <sup>8</sup> and  $Mg(pc)$ <sup>9</sup> (especially for the imidazole complexes), the energies of these transitions vary by 2 000 or 3 000  $cm^{-1}$ . For the  $NiL$  monomer, we assign the band at 36 286  $cm^{-1}$  as an  $N$  band.

(5) *Exciton Coupling between the Rings in the Dimer.*—Figure 12 shows a qualitative orbital diagram that represents the effects of exciton coupling to be expected with a dimer of geometry  $D_{4h}$ . The exciton coupling results in pairs of states, the two lowest being  $Q^-(E_g)$  and  $Q^+(E_u)$ , and  $B^-(E_g)$  and  $B^+(E_u)$ , where transitions to the  $E_u$  states are allowed, while transitions to  $E_g$  are forbidden.<sup>13</sup> No orbital overlap or additional vibronic coupling is assumed. The strictly forbidden transitions in  $D_{4h}$  symmetry may gain some intensity upon a change to a number of lower symmetries, for example, to  $C_{2v}$  symmetry. The picture becomes more complicated when the orbital overlap and additional vibronic coupling effects are added. A similar scheme is used by Dodsworth *et al.*<sup>12</sup> to account for the  $Q$ -band region spectra of binuclear neopentoxypthalocyanines. Because the spectral data for our systems are rather better resolved we feel that we can associate individual bands with each of the two components predicted for the  $Q$ -band region. However, as for the situation for the  $\alpha$  polymorphic metal phthalocyanines,<sup>4</sup> the  $B$ -band region remains problematical.

### Conclusions

The m.c.d. spectra recorded for the monomeric crown-pc species indicate that the peripheral crown substituent results in a significant lowering of the energy of the second excited degenerate state, the  $B$  band. As in previous work, analysis of the complicated spectral envelope that is observed between 400 and 220 nm requires the combination of absorption and m.c.d. data. Bands at 14 946, 24 398, 31 414, and 36 286  $\text{cm}^{-1}$  are assigned to the  $Q$ ,  $B_1$ ,  $B_2$ , and  $N$  bands of the pc ring. M.c.d. spectra of the dimeric  $H_2L$  species confirm previous observations that one of the major effects of dimerization is to increase the symmetry of the  $\pi$  states from the  $D_{2h}$  of the monomer to at least  $D_{4h}$ , so that  $A$  terms are observed under the main  $\pi \rightarrow \pi^*$  transitions in the spectra of the metal-free dimer. Deconvolution of the absorption and m.c.d. spectra of the dimeric NiL and  $H_2L$  species shows that split pairs of bands are observed for the  $Q$  and  $B$  bands, giving rise to pairs of m.c.d.  $A$  terms. The splitting is interpreted in terms of exciton coupling in the dimer species. The separation for the  $Q$ -band components is of the order 1 000  $\text{cm}^{-1}$  (Ni, 950  $\text{cm}^{-1}$ ), while the separation of the  $B$ -band components is about 2 000  $\text{cm}^{-1}$  (Ni, 2 180,  $H_2$ , 1 925  $\text{cm}^{-1}$ ).

### Acknowledgements

The authors gratefully acknowledge the financial support of this work by the Natural Sciences and Engineering Research Council of Canada through grants under the Operating and Equipment programme, and from the Academic Development

Fund at the University of Western Ontario (to M. J. S.); N. K. acknowledges the hospitality of Professor A. B. P. Lever at York University and thanks the Department of Chemistry, York University, Ontario for study leave (permanent address: Pharmaceutical Institute, Tohoku University, Sendai 980, Japan). Z. G. and M. J. S. are associated with the Centre of Chemical Physics at the University of Western Ontario.

### References

- 1 C. Ercolani, C. Neri, and P. Porta, *Inorg. Chim. Acta*, 1967, **1**, 415.
- 2 E. A. Lucia and F. O. Verderame, *J. Chem. Phys.*, 1968, **48**, 2674.
- 3 B. H. Schechtman and W. E. Spicer, *J. Mol. Spectrosc.*, 1970, **33**, 28.
- 4 B. R. Hollebome and M. J. Stillman, *J. Chem. Soc., Faraday Trans. 2*, 1978, 2107.
- 5 E. Cilberto, K. A. Doris, W. J. Pietro, G. M. Reisner, D. E. Ellis, I. Fragala, F. H. Herbstein, M. A. Ratner, and T. J. Marks, *J. Am. Chem. Soc.*, 1984, **106**, 7748.
- 6 N. Kobayashi and Y. Nishiyama, *J. Chem. Soc., Chem. Commun.*, 1986, 1462.
- 7 N. Kobayashi and A. B. P. Lever, *J. Am. Chem. Soc.*, 1987, **26**, 1087.
- 8 T. Nyokong, Z. Gasyna, and M. J. Stillman, *Inorg. Chem.*, 1987, **26**, 1087.
- 9 E. Ough, T. Nyokong, K. A. Creber, and M. J. Stillman, *Inorg. Chem.*, 1988, **27**, 2724.
- 10 W. R. Browett and M. J. Stillman, *Comput. Chem.*, 1987, **11**, 241.
- 11 N. S. Hush and I. S. Woolsey, *Mol. Phys.*, 1971, **21**, 465.
- 12 E. S. Dodsworth, A. B. P. Lever, P. Seymour, and C. C. Leznoff, *J. Phys. Chem.*, 1985, **89**, 5698.
- 13 M. Gouterman, D. Holten, and E. Lieberman, *Chem. Phys.*, 1977, **25**, 139.
- 14 Z. Gasyna, W. R. Browett, T. Nyokong, R. Kitchenham, and M. J. Stillman, *Chemom. Intellig. Lab. Syst.*, in the press.
- 15 P. N. Schatz, R. L. Mowery, and E. R. Krausz, *Mol. Phys.*, 1978, **35**, 1537.
- 16 S. B. Piepho and P. N. Schatz, 'Group Theory in Spectroscopy, with Application to Magnetic Circular Dichroism,' Wiley, New York, 1982.
- 17 W. R. Browett and M. J. Stillman, *Comput. Chem.*, 1987, **11**, 73.
- 18 M. Gouterman, in 'The Porphyrins,' ed. D. Dolphin. Academic Press, New York, 1978, vol. 3, part A, pp. 1—165.
- 19 A. J. McHugh, M. Gouterman, and C. Weiss, *Theor. Chim. Acta*, 1972, **24**, 346.
- 20 K. A. Martin and M. J. Stillman, *Can. J. Chem.*, 1979, **57**, 1111.
- 21 M. J. Stillman and A. J. Thomson, *J. Chem. Soc., Faraday Trans. 2*, 1974, 805.
- 22 M. J. Stillman and A. J. Thomson, *J. Chem. Soc., Faraday Trans. 2*, 1974, 790.
- 23 P. J. Stephens, R. L. Mowery, and P. N. Schatz, *J. Chem. Phys.*, 1971, **55**, 224.
- 24 P. J. Stephens, *Chem. Phys. Lett.*, 1968, **2**, 241.
- 25 B. R. Hollebome and M. J. Stillman, *Chem. Phys. Lett.*, 1974, **29**, 284.

Received 18th November 1988; Paper 8/04594A